Inorg. Chem. **2007**, *46*, 10781–10790

Amine-Templated Open-Framework Zinc Arsenates of Varying Dimensionalities: Synthesis, Structure, Polymorphism, and Transformation Reactions

V. Koteswara Rao, Sandip Chakrabarti, and Srinivasan Natarajan*

Framework Solids Laboratory, Solid State and Structural Chemistry Unit, Indian Institute of Science, Bangalore-560 012, India

Received July 23, 2007

Eight new open-framework zinc arsenates, encompassing the entire hierarchy of open-framework structures, have been prepared hydrothermally. The structures include zero-dimensional, one-dimensional chains, two-dimensional layers, and three-dimensional structures formed through the transformation of the molecular zinc arsenates. The structure of $[C_6N_4H_{21}][Zn(HAsO_4)_2(H_2AsO_4)]$, **I**, is composed of ZnO_4 and H_2AsO_4 units connected through the vertices forming four-membered rings with $HAsO_4$ units hanging from the Zn center. The four-membered rings are connected through the corners forming the one-dimensional chain structures in $[C_4N_2H_{12}][Zn(HAsO_4)_2]\cdot H_2O$, **II**, and $[C_5N_2H_{14}][Zn(HAsO_4)_2]\cdot H_2O$, **III**. ZnO_4 and AsO_4 units form a fully four-connected two-dimensional structure in $[C_4N_2H_{12}][Zn(AsO_4)]_2$, **IV**. One-dimensional zigzag ladders are connected through $HAsO_4$ units forming two-dimensional layers in $[C_4N_2H_{12}]_{1.5}[Zn_2(AsO_4)(HAsO_4)_2]\cdot H_2O$, **V**, while the similar building units form a layer with hanging $HAsO_4$ units in the layered arsenate $[C_6N_4H_{21}]_6[Zn_{12}(HAsO_4)_{21}]$, **VI**. Hanging $HAsO_4$ units are also observed in the polymorphic structures of $[C_6N_3H_{20}][Zn_2(AsO_4)(HAsO_4)_2]\cdot 2H_2O$, **VII** and **VIII**. Formation of zero-dimensional monomer, **I**, a fully four-connected layer, **IV**, and the polymorphic structures, **VII** and **VIII**, are important and noteworthy. The transformation reactions of **I** indicate that the monomer is reactive and gives rise to structures of higher dimensionalities, indicating a possible Aufbau-type building-up process in these structures.

Introduction

Inorganic compounds possessing open-framework structures continue to be attractive for their many properties, both potential as well as actual.[1] Of the many compounds that have been prepared and characterized, the phosphate-based structures are the dominant class. There have been considerable synthetic efforts to study systems involving other anions. This has resulted in the discovery of many new families of compounds based on phosphites,[2] arsenates,[3] sulfates,[4] and selenates.[5] We have been interested in the study of arsenate-based frameworks for the following reasons. (i) Arsenic belongs to the same group as phosphorus and chemically behaves similarly. (ii) As^{5+} is larger (0.335 Å) compared to P^{5+} (0.17 Å), which can result in novel frameworks. (iii) The pK_a values of H_3PO_4 and H_3AsO_4 are comparable (pK_{a1} = 2.12, pK_{a2} = 7.21, pK_{a3} = 12.32 for H_3PO_4; pK_{a1} = 2.3, pK_{a2} = 6.9, pK_{a3} = 11.5 for H_3AsO_4), though the arsenic acid is somewhat weaker.

Though it is easy to visualize the close similarities between the phosphate and the arsenate anions, a search of the available literature clearly indicates that the number of open-framework arsenates is not many. Amine-templated arsenate frameworks have been isolated with Al,[6] Ga,[7] V,[8] Fe,[9] Zn,[10] and Mo.[11] These compounds exhibit a wide variety of compositions and diversity in their structures. We have been

* To whom correspondence should be addressed. E-mail: snatarajan@sscu.iisc.ernet.in.

(1) Cheetham, A. K.; Ferey, G.; Loiseau, T. *Angew. Chem., Int. Ed.* **1999**, *38*, 3268.
(2) Liang, J.; Wang, Y.; Yu, J.; Li, L.; Xu, R. *Chem. Commun.* **2003**, 882.
(3) (a) Chakrabarti, S.; Natarajan, S. *Dalton Trans.* **2002**, 3874. (b) Chakrabarti, S.; Natarajan, S. *Dalton Trans.* **2002**, 4156.
(4) (a) Rao, C. N. R.; Behera, J. N.; Dan, M. *Chem. Soc. Rev.* **2006**, *35*, 375. (b) Behera, J. N.; Rao, C. N. R. *J. Am. Chem. Soc.* **2006**, *128*, 9334.
(5) (a) Feng, M. L.; Mao, J. G.; Song, J. L. *J. Solid State Chem.* **2004**, *177*, 3529. (b) Behera, J. N.; Ayi, A. A.; Rao, C. N. R. *Chem. Commun.* **2004**, 968. (c) Udayakumar, D.; Dan, M.; Rao, C. N. R. *Eur. J. Inorg. Chem.* **2004**, 1733.
(6) (a) Yang, G.; Li, L.; Chen, J.; Xu, R. *Chem. Commun.* **1989**, 810. (b) Chen, J.; Xu, R. *J. Solid State Chem.* **1990**, *87*, 152. (c) Li, L.; Wu, L. *Acta Crystallogr., Sect. C* **1991**, *47*, 246.

10.1021/ic7014594 CCC: $37.00
Published on Web 11/14/2007

Table 1. Synthesis Conditions Employed for the Zinc Arsenates **I**−**VIII**[a]

no.	composition	temp (°C)	time (h)	pH (initial, final)	product	yield (%)
1	$1ZnO + 2HCl + 2CH_3COOH + 2As_2O_5 + 2TREN + (22THF + 200H_2O)$	75, 110	72, 24	4.0, 4.0	$[C_6N_4H_{21}][Zn(HAsO_4)_2(H_2AsO_4)]$, **I**	80
2	$1Zn(OAc)_2{\cdot}2H_2O + 2\ As_2O_5 + 6PIP + 400H_2O$	115	192	8.0, 8.0	$[C_4N_2H_{12}][Zn(HAsO_4)_2]{\cdot}H_2O$, **II**	65[b]
3	$1ZnO + 2CH_3COOH + 4.9Homopip + 2As_2O_5 + (22THF + 200H_2O)$	75	72	6.0, 7.0	$[C_5N_2H_{14}][Zn(HAsO_4)_2]{\cdot}H_2O$, **III**	75
4	$1Zn(OAc)_2{\cdot}2H_2O + 2As_2O_5 + 6PIP + 400H_2O$	125	72	8.0, 9.0	$[C_4N_2H_{12}][Zn(AsO_4)]_2$, **IV**	80
5	$1Zn(OAc)_2{\cdot}2H_2O + 2As_2O5 + 4PIP + 400H_2O$	125	120	6.0, 7.0	$[C_4N_2H_{12}]_{1.5}[Zn_2(AsO_4)(HAsO_4)_2]{\cdot}H_2O$, **V**	70[b]
6	$1ZnO + 3CH_3COOH + 2As_2O_5 + 2TREN + (22THF + 200H_2O)$	125	120	6.0	$[C_6N_4H_{21}]_6[Zn_{12}(HAsO_4)_{21}]$, **VI**	80
7	$1ZnO + 2HCl + 2As_2O_5 + CH_3COOH + 2DPTA + (22THF + 200H_2O)$	75, 150	72, 24	7.0	$[C_6N_3H_{20}][Zn_2(AsO_4)(HAsO_4)_2]{\cdot}2H_2O$, **VII**	75
8	$1ZnO + 2As_2O_5 + 3CH_3COOH + 2DPTA + (22THF + 200H_2O)$	75, 150	72, 24	7.0	$[C_6N_3H_{20}][Zn_2(AsO_4)(HAsO_4)_2]{\cdot}2H_2O$, **VIII**	75

[a] Where TREN = tris(2-aminoethyl)amine, PIP = piperazine, Homopip = homopiperazine, DPTA = 3,3′-diaminodipropylamine. [b] Mixed phase: contains single crystals and uncharacterized powder phase.

investigating the formation of zinc arsenate structures in the presence of organic amines, employing mild hydro/solvothermal conditions. Our efforts have yielded zinc arsenate structures with zero-, one-, and two-dimensionally extended structures.

The zinc arsenates $[C_6N_4H_{21}][Zn(HAsO_4)_2(H_2AsO_4)]$, **I**, $[C_4N_2H_{12}][Zn(HAsO_4)_2]{\cdot}H_2O$, **II**, $[C_5N_2H_{14}][Zn(HAsO_4)_2]{\cdot}H_2O$, **III**, $[C_4N_2H_{12}][Zn(AsO_4)]_2$, **IV**, $[C_4N_2H_{12}]_{1.5}[Zn_2(AsO_4)(HAsO_4)_2]{\cdot}H_2O$, **V**, $[C_6N_4H_{21}]_6[Zn_{12}(HAsO_4)_{21}]$, **VI**, and $[C_6N_3H_{20}][Zn_2(AsO_4)(HAsO_4)_2]{\cdot}2H_2O$, **VII** and **VIII**, have been prepared employing mild reaction conditions. In addition to the isolation of these structures we also attempted a few transformation reactions, particularly on the zero-dimensional compound. Formation of two polymorphic two-dimensional structures **VII** and **VIII** along with isolation of the first zero-dimensional zinc arsenate **I** is noteworthy. In this paper, we present the synthesis, structure, polymorphism, and transformation studies for the zinc arsenate phases.

Experimental Section

Synthesis and Initial Characterization. All compounds isolated in the present study were synthesized in the presence of organic amines employing mild hydro/solvothermal reactions in the temperature range 75−150 °C in Teflon-lined acid-digestion autoclaves. All chemicals were purchased from Aldrich and used without further purification. The general purity of the chemicals is >99.0%. The compositions of the reaction mixtures and conditions employed for the synthesis are given in Table 1. In a typical experiment, for the synthesis of **I** 0.2528 g of As_2O_5 was added to a mixture of H_2O (2 mL) and THF (1 mL). To this 0.452 g of ZnO, 0.1 mL of HCl (35.5%), and 0.06 mL of CH_3COOH were added under continuous stirring. Finally, 0.17 mL of TREN (tris(2-aminoethyl)amine) was added, and the mixture was homogenized for 30 min at room temperature. The final reaction mixture with the composition $1ZnO:2HCl:2CH_3OOH:2As_2O_5:2TREN:(22THF + 200H_2O)$ was taken in a 7 mL Teflon-lined acid-digestion autoclave and heated at 75 °C for 72 h followed by heating at 110 °C for 24 h. The initial pH of the reaction mixture was ∼4.0, which did not show any appreciable change after the reaction. The product containing good-quality colorless single crystals in good yields (Table 1) was filtered and washed with distilled water and dried at ambient conditions. Initial characterizations were carried out using powder XRD, elemental analysis, IR, and TGA studies. The powder XRD patterns (Philips X'Pert, Pro) of compounds **II** and **V** showed some minor impurity peaks, and in spite of our repeated attempts, we were not able to prepare the pure phases; hence, other than the single-crystal structure, we have not been able to characterize these compounds completely. The XRD patterns of all remaining compounds indicated that the patterns were new and entirely consistent with the XRD patterns simulated based on the structure determined using the single-crystal X-ray diffraction.

Elemental analyses of the crystals were carried out using a Thermo Finnigan FLASH EA 1112 CHNS analyzer. Anal. Calcd for **I**: C, 11.34; H, 3.96; N, 8.81. Found: C, 11.29; H, 4.27; N, 8.55. Anal. Calcd for **III**: C, 12.90; H, 3.89; N, 6.01. Found: C, 12.82; H, 4.17; N, 6.56. Anal. Calcd for **IV**: C, 9.67; H, 2.43; N, 5.64. Found: C, 9.84; H, 2.81; N, 6.01. Anal. Calcd for **VI**: C, 9.36; H, 3.2; N, 7.27. Found: C, 9.37; H, 3.42; N, 7.14. Anal. Calcd for **VIII**: C, 10.0; H, 3.64; N, 5.83. Found: C, 10.56; H, 3.75; N, 6.32.

IR spectroscopic studies (Perkin-Elmer, SPECTRUM 1000) were carried out as a KBr pellet in the range 400−4000 cm^{-1} for all compounds. The spectra exhibited typical peaks corresponding to the lattice water, amine molecule, and arsenate moiety. The observed bands are $\nu_{(H2O)}$ = 3500−3600 cm^{-1}, $\nu_{(N-H)}$ = 3200−3400 cm^{-1}, $\nu_{(C-H)}$ = 2800−3090 cm^{-1}, $\delta_{(H2O)}$ = 1610−1625 cm^{-1}, $\delta_{(N-H)}$ = 500−1600 cm^{-1}, $\delta_{(C-H)}$ = 1300−1500 cm^{-1}, $\nu_{(As-OH)}$ =

(7) (a) Chen, J.; Li, L.; Yang, G.; Xu, R. *Chem. Commun.* **1989**, 1217. (b) Liao, Y. C.; Luo, S. H.; Wang, S. L.; Kao, H. M.; Lii, K. H. *J. Solid State Chem.* **2000**, *155*, 37. (c) Luo, S. H.; Jiang, Y. C.; Wang, S. L.; Kao, H. M.; Lii, K. H. *Inorg. Chem.* **2001**, *40*, 5381. (d) Chen, C. Y.; Lii, K. H.; Jacobson, A. J. *J. Solid State Chem.* **2003**, *172*, 252. (e) Loiseau, T.; Ferey, G. *Acta Crystallogr., Sect. C* **2004**, *60*, i30.

(8) (a) Haushalter, R. C.; Wang, Z.; Meyer, L. M.; Dhingra, S. S.; Thomson, M. E.; Zubieta, J. *Chem. Mater.* **1994**, *6*, 1463. (b) Liu, A. H.; Wang, S. L. *Inorg. Chem.* **1998**, *37*, 3415. (c) Huang, L. H.; Kao, H. M.; Lii, K. H. *Inorg. Chem.* **2002**, *41*, 2936.

(9) (a) Ekambaram, S.; Sevov, S. C. *Inorg. Chem.* **2000**, *39*, 2405. (b) Bazan, B.; Mesa, J. L.; Pizarro, J. L.; Lezama, L.; Arriortua, M. I.; Rojo, T. *Inorg. Chem.* **2000**, *39*, 6056. (c) Bazan, B.; Mesa, J. L.; Pizarro, J. L.; Goni, A.; Lezama, L.; Arriortua, M. I.; Rojo, T. *Inorg. Chem.* **2001**, *40*, 5691. (d) Chakrabarti, S.; Natarajan, S. *Angew. Chem., Int. Ed.* **2002**, *41*, 1224. (e) Chakrabarti, S.; Pati, S. K.; Green, M. A.; Natarajan, S. *Eur. J. Inorg. Chem.* **2003**, 3820. (f) Chakrabarti, S.; Pati, S. K.; Green, M. A.; Natarajan, S. *Eur. J. Inorg. Chem.* **2004**, 3846. (g) Bazan, B.; Mesa, J. L.; Pizarro, J. L.; Fernandez, J. R.; Marcos, J. S.; Roig, A.; Molins, E.; Arriortua, M. I.; Rojo, T. *Chem. Mater.* **2004**, *16*, 5249. (h) Rao, V. K.; Natarajan, S. *Mater. Res. Bull.* **2006**, *41*, 973.

(10) (a) Bu, X.; Gier, T. E.; Stucky, G. D. *Chem. Commun.* **1997**, 2271. (b) Bu, X.; Feng, P.; Gier, T. E.; Stucky, G. D. *J. Solid State Chem.* **1998**, *136*, 210. (c) Gier, T. E.; Bu, X.; Feng, P.; Stucky, G. D. *Nature* **1998**, *395*, 154. (d) Harrison, W. T. A.; Phillips, M. L. F.; Chavez, A. V.; Nenoff, T. M. *J. Mater. Chem.* **1999**, *9*, 3087. (e) Hajem, A. A.; Trojette, B.; Driss, A.; Jouini, T. *Acta Crystallogr., Sect. C* **2000**, *56*, 793. (f) Kongshaug, K. O. *Acta Crystallogr., Sect. C* **2000**, *56*, e503. (g) Chakrabarti, S.; Natarajan, S. *Dalton Trans.* **2002**, 3874. (h) Chakrabarti, S.; Natarajan, S. *Dalton Trans.* **2002**, 4156. (i) Wiggin, S. B.; Teller, M. A. *Chem. Commun.* **2006**, 1100.

(11) (a) Wang, S. L.; Hsu, K. F.; Nieh, Y. P. *Dalton Trans.* **1994**, 1681. (b) Lee, M. Y.; Wang, S. L. *Chem. Mater.* **1999**, *11*, 3588. (c) Sun, C.; Li, Y.; Wang, E.; Xiao, D.; An, H.; Xu, L. *Inorg. Chem.* **2007**, *46*, 1563.

1100−1200, $\nu_{(C-N)} = 1000-1100\ cm^{-1}$, $\nu_{as(As-O)} = 760-960\ cm^{-1}$, $\nu_{s(As-O)} = 660-740\ cm^{-1}$.

TGA studies (Mettler-Toledo TG850) of compounds **I**, **III**, and **VI**−**VIII** were carried out in an atmosphere of flowing oxygen (flow rate = 100 mL min^{-1}) in the temperature range 25−850 °C (heating rate = 5 °C min^{-1}). The results indicate that there is a sharp weight loss at 300 and 375 °C for **I** and **VI** followed by a long tail up to 600 °C. The total observed weight loss of 81% and 70% for **I** and **VI**, respectively, corresponds to loss of the organic amine, condensation of terminal −OH groups, and loss of arsenic from the system (calcd 83% for **I** and 75% for **VI**). The calcined phases are poorly crystalline with XRD lines corresponding to ZnO (ICDD-36-1451). The results for **III** indicate a weight loss of 4% at 100 °C, which corresponds to loss of water molecules (calcd 3.9%). The second weight loss of 76% at 250 °C with a long tail up to 600 °C corresponds to loss of amine molecules, condensation of the −OH groups, and loss arsenic from the system (calcd 78.5%). The calcined phase is poorly crystalline with the XRD lines corresponding to ZnO (ICDD-36-1451). The TGA studies of the polymorphic arsenates **VII** and **VIII** appear to be different with **VII** showing long tails up to 600 °C. An initial weight loss of ∼6% observed in the range 60−200 °C corresponds to loss of adsorbed and lattice water (calcd 5%). The continuous weight loss of 55.5% in the range 240−600 °C corresponds to loss of the amine, condensation of −OH, and partial loss of arsenic (calcd 51.2%). The powder XRD of the calcined sample was a mixture of ZnO (ICDD-36-1451) and $Zn_2As_2O_7$ (ICDD-01-0798). In the case of **VIII**, the initial weight loss of ∼4% in the range 25−250 °C corresponds to loss of adsorbed and lattice water (calcd 5%). The continuous weight loss of ∼85% in the range 250−800 °C corresponds to loss of amine, condensation of −OH, and complete loss of arsenic (calcd 78%). It is clear that removal of the amine molecules in all cases leads to a collapse of the framework structure and results in a situation wherein further characterizations through adsorption and related studies could not be performed. The powder XRD of the calcined sample reveals that it is amorphous.

Single-Crystal Structure Determination. A suitable colorless single crystal of each compound was carefully selected under a polarizing microscope and glued to a thin glass fiber with a cyanoacrylate (superglue) adhesive. The single-crystal diffraction data were collected on a Bruker AXS Smart Apex CCD diffractometer at 293(2) K. The X-ray generator was operated at 50 kV and 35 mA using Mo Kα (λ = 0.71073 Å) radiation. Data were collected with a ω scan width of 0.3°. A total of 606 frames were collected in different settings of ϕ keeping the sample-to-detector distance fixed at 6.0 cm and the detector position (2θ) fixed at −25°. Pertinent experimental details of the structure determination of each compound are listed in Table 2. Data were reduced using SAINTPLUS,[12] and an empirical absorption correction was applied using the SADABS program.[13] The crystal structure was solved and refined by direct methods using SHELXL97[14] present in the WinGx suit of program (Version 1.63.04a).[15] The hydrogen atoms of the lattice water molecule present in **VIII** were not located. We made use of bond valence sum calculations[16] to determine the oxygens, which could be hydroxyl groups. The hydrogen positions

Table 2. Crystal Data and Structure Refinement Parameters for **I**−**VIII**[a]

structural parameter	**I**	**II**	**III**	**IV**	**V**	**VI**	**VII**	**VIII**
empirical formula	$As_3ZnO_{12}H_{25}N_4C_6$	$As_2ZnO_9H_{16}N_2C_4$	$As_2ZnO_9H_{18}N_2C_5$	$As_1ZnO_4H_6NC_2$	$As_3Zn_2O_{13}H_{22}N_3C_6$	$As_{21}Zn_{12}O_{84}H_{147}N_{24}C_{36}$	$As_3Zn_2O_{14}H_{26}N_3C_6$	$As_3Zn_2O_{14}H_{26}N_3C_6$
fw	635.43	451.40	465.42	496.75	699.77	4618.54	719.80	719.78
cryst syst	orthorhombic	monoclinic	triclinic	monoclinic	monoclinic	triclinic	triclinic	triclinic
space group	*Pbca* (No. 61)	$P2_1/n$ (No. 14)	*P*-1 (No. 2)	$P2_1/n$ (No. 14)	$P2_1/c$ (No. 14)	*P*-1 (No. 2)	*P*-1 (No. 2)	*P*-1 (No. 2)
a (Å)	12.515(2)	9.1330(3)	8.4928(12)	9.2191(12)	8.3767(6)	18.687(4)	9.0673(7)	8.5375(3)
b (Å)	14.985(2)	14.3268(3)	8.6322(12)	6.0024(8)	26.346(2)	18.722(4)	9.3326(7)	8.7645(3)
c (Å)	20.056(3)	9.4993(2)	10.1873(14)	11.0228(14)	8.5676(6)	19.631(5)	12.7863(9)	14.1028(5)
α (deg)	90.000	90.000	87.198(2)	90.000	90.000	90.936(4)	87.515(12)	98.478(6)
β (deg)	90.000	96.5870(10)	78.423(2)	114.717	111.573(10)	92.545(4)	81.109(11)	90.742(6)
γ (deg)	90.000	90.000	65.997(2)	90.000	90.000	118.872(4)	72.574(11)	101.834(6)
V (Å^3)	3761.30(10)	1234.38(5)	667.94(16)	554.08(12)	1758.3(2)	6003(2)	1019.93(13)	1020.54(7)
Z	8	4	2	4	4	2	2	2
D (calcd/g cm^{-3})	2.244	2.429	2.314	2.747	2.643	2.555	2.344	2.336
μ (mm^{-1})	6.609	7.352	6.797	12.764	8.404	8.218	7.251	7.247
λ (Mo Kα/Å)	0.71073	0.71073	0.71073	0.71073	0.71073	0.71073	0.7107 3	0.71073
θ range (deg)	2.03−28.04	2.58−23.26	2.04−27.35	2.43−23.28	1.55−23.31	1.57−28.04	2.29−28.10	1.46−28.16
total data collected	30 911	4995	5170	2203	2535	70 120	11 070	11 504
unique data	4445	1763	2685	800	1882	27 765	4605	4717
R indexes	$R_1 = 0.0330$;	$R_1 = 0.0367$;	$R_1 = 0.0423$;	$R_1 = 0.0439$;	$R_1 = 0.0444$;	$R_1 = 0.0631$;	$R_1 = 0.0527$;	$R_1 = 0.0507$;
$[I > 2\sigma(I)]$	$wR_2 = 0.0671$	$wR_2 = 0.0934$	$wR_2 = 0.1236$	$wR_2 = 0.1126$	$wR_2 = 0.0951$	$wR_2 = 0.1095$	$wR_2 = 0.1327$	$wR_2 = 0.1467$
R indexes	$R_1 = 0.0512$;	$R_1 = 0.0448$;	$R_1 = 0.0450$;	$R_1 = 0.0500$;	$R_1 = 0.0754$;	$R_1 = 0.1076$;	$R_1 = 0.0613$;	$R_1 = 0.0605$;
(all data)	$wR_2 = 0.0726$	$wR_2 = 0.1000$	$wR_2 = 0.1260$	$wR_2 = 0.1204$	$wR_2 = 0.1261$	$wR_2 = 0.1255$	$wR_2 = 0.1389$	$wR_2 = 0.1565$

[a] $R_1 = \sum||F_0| - |F_c||/\sum|F_0|$; $wR_2 = \{\sum[w(F_0^2 - F_c^2)^2]/\sum[w(F_0^2)^2]\}^{1/2}$; $w = 1/[\sigma^2(F_0)^2 + (aP)^2 + bP]$, $P = [\max(F_0^2,0) + 2(F_c)^2]/3$, where $a = 0.0313$ and 3.6713 for **I**, $a = 0.0377$ and $b = 5.0069$ for **II**, $a = 0.0830$ and 0.8181 for **III**, $a = 0.0485$ and $b = 0.4647$ for **IV**, $a = 0.0551$ and $b = 0.000$ for **V**, $a = 0.0250$ and $b = 17.9490$ for **VI**, $a = 0.0948$ and $b = 0.000$ for **VII**, and $a = 0.0970$ and $b = 0.000$ for **VIII**.

(12) *SMART* (V 5.628), *SAINT* (V 6.45a), *XPREP*, *SHELXTL*; Bruker AXS Inc.: Madison, WI, 2004.

(13) Sheldrick, G. M. *Siemens Area Detector Absorption Correction Program*; University of Göttingen: Göttingen, Germany, 1994.

(14) Sheldrick, G. M. *SHELXL-97 Program for Crystal Structure Solution and Refinement*; University of Göttingen: Göttingen, Germany, 1997.

(15) Farrugia, J. L. *J. Appl. Crystallogr.* **1999**, *32*, 837.

(16) Brown, I. D.; Altermatt, D. *Acta Crystallogr., Sect. B* **1985**, *41*, 244.

Table 3. Important Bond Distances Observed in Selected Zinc Arsenates: **I**, **IV**, **V**, **VII**, and **VIII**[a]

bond	distance, Å	bond	distance, Å
	compound **I**		
As(1)−O(1)	1.661(2)	As(3)−O(9)	1.6565(12)
As(1)−O(2)	1.668(2)	As(3)−O(10)	1.6694(11)
As(1)−O(3)	1.674(2)	As(3)−O(11)	1.6738(12)
As(1)−O(4)	1.727(2)	As(3)−O(12)	1.7125(12)
As(2)−O(5)#1	1.647(3)	Zn(1)−O(10)	1.9118(12)
As(2)−O(6)	1.658(3)	Zn(1)−O(5)	1.921(3)
As(2)−O(7)	1.6792(12)	Zn(1)−O(6)	1.944(3)
As(2)−O(8)	1.6981(11)	Zn(1)−O(2)#2	1.947(3)
	compound **IV**		
As(1)−O(1)	1.677(5)	Zn(1)−O(1)#1	1.936(5)
As(1)−O(2)	1.677(5)	Zn(1)−O(2)#2	1.953(4)
As(1)−O(3)	1.693(4)	Zn(1)−O(3)#3	1.959(4)
As(1)−O(4)	1.706(4)	Zn(1)−O(4)	2.005(5)
	compound **V**		
As(1)−O(1)	1.649(7)	As(3)−O(11)	1.679(7)
As(1)−O(2)	1.677(6)	As(3)−O(12)	1.718(7)
As(1)−O(3)	1.684(6)	Zn(1)−O(1)#1	1.942(7)
As(1)−O(4)	1.723(7)	Zn(1)−O(2)	2.001(7)
As(2)−O(5)	1.678(7)	Zn(1)−O(5)	1.970(7)
As(2)−O(6)	1.696(7)	Zn(1)−O(7)#1	1.922(7)
As(2)−O(7)	1.678(7)	Zn(2)−O(3)#2	1.966(7)
As(2)−O(8)	1.699(7)	Zn(2)−O(6)	1.961(7)
As(3)−O(9)	1.657(7)	Zn(2)−O(9)#3	1.966(7)
As(3)−O(10)	1.669(7)	Zn(2)−O(11)	1.944(7)
	compound **VII**		
As(1)−O(1)	1.665(4)	As(3)−O(11)	1.691(4)
As(1)−O(2)	1.671(4)	As(3)−O(12)	1.695(4)
As(1)−O(3)	1.689(4)	Zn(1)−O(9)	1.940(4)
As(1)−O(4)	1.723(4)	Zn(1)−O(3)	1.947(4)
As(2)−O(5)	1.665(5)	Zn(1)−O(12)#1	1.958(4)
As(2)−O(7)	1.666(4)	Zn(1)−O(2)#2	1.966(4)
As(2)−O(6)	1.681(4)	Zn(2)−O(10)#3	1.938(4)
As(2)−O(8)	1.719(4)	Zn(2)−O(1)#4	1.945(4)
As(3)−O(9)	1.681(4)	Zn(2)−O(11)	1.964(4)
As(3)−O(10)	1.690(4)	Zn(2)−O(7)	1.970(4)
	compound **VIII**		
As(1)−O(1)	1.659(4)	As(3)−O(12)	1.686(4)
As(1)−O(3)	1.678(4)	As(3)−O(11)	1.686(4)
As(1)−O(2)	1.682(5)	Zn(1)−O(6)	1.929(4)
As(1)−O(4)	1.717(5)	Zn(1)−O(11)	1.942(4)
As(2)−O(5)	1.664(4)	Zn(1)−O(12)#2	1.961(4)
As(2)−O(6)#1	1.666(4)	Zn(1)−O(5)	1.975(4)
As(2)−O(7)#1	1.691(4)	Zn(2)−O(9)	1.940(4)
As(2)−O(8)	1.698(4)	Zn(2)−O(7)	1.941(4)
As(3)−O(9)	1.671(4)	Zn(2)−O(10)#3	1.944(4)
As(3)−O(10)	1.681(4)	Zn(2)−O(13)	1.944(5)

[a] Symmetry transformations used to generate equivalent atoms. **I**: #1 $x + 1/2, y, -z + 1/2$; #2 $-x + 2, -y + 2, -z + 1$. **IV**: #1 $-x + 1/2, y - 1/2, -z + 1/2$; #2 $-x, -y, -z$; #3 $x, y, -1$. **V**: #1 $x, -y + 3/2, z - 1/2$; #2 $x, -y + 3/2, z + 1/2$; #3 $-x, -y + 2, -z + 1$, **VII**: #1 $-x + 1, -y + 1, -z$; #2 $-x, -y + 1, -z$; #3 $-x + 1, -y + 2, -z$; #4 $x, y + 1, z$. **VIII**: #1 $-x + 1, -y + 1, -z$; #2 $-x + 1, -y, -z$; #3 $-x, -y, -z$.

observed in the difference Fourier maps were also in agreement with the bond valence calculations. The idealized hydrogen positions were then placed geometrically and refined using the riding mode. The last cycles of refinements included atomic positions, anisotropic thermal parameters for all non-hydrogen atoms, and isotropic thermal parameters for all hydrogen atoms. Full-matrix least-squares structure refinement against $|F^2|$ was carried out using the SHELXL package of programs.[14,15] Selected bond distances are listed in Table 3 and Table S1. Important hydrogen-bond distances are listed in Table 4 and Table S2. Crystallographic data (excluding structure factors) have been deposited with CCDC numbers 654239−654246. These data can be obtained free of charge from the Cambridge Crystallographic Data Centre (CCDC) via www.ccdc.cam.ac.uk/data_request/cif.

Table 4. Important Hydrogen-Bond Interactions Observed in **I**, **IV**, **V**, **VII**, and **VIII**

D−H···A	D−H (A)	H···A (Å)	D···A (Å)	D−H···A (deg)
		compound **I**		
N(2)−H(1)···O(1)	0.89	1.92	2.776(3)	161
N(2)−H(3)···O(9)	0.89	2.09	2.979(16)	175
O(4)−H(4)···O(11)	0.82	1.95	2.690(3)	149
O(7)−H(7)···O(11) intra	0.82	1.68	2.488(15)	167
O(8)−H(8)···O(3)	0.82	1.77	2.555(3)	158
O(12)−H(12)···O(3)	0.82	1.88	2.645(3)	155
N(3)−H(18)···O(1)	0.89	2.01	2.869(4)	162
N(3)−H(19)···O(3)	0.89	1.92	2.741(4)	153
N(3)−H(20)···O(9)	0.89	2.09	2.943(3)	160
N(4)−H(23)···O(9)	0.89	1.80	2.673(4)	165
C(1)−H(1)···O(5)	0.97	2.46	3.428(5)	173
C(4)−H(13) ···O(5)	0.97	2.46	3.367(5)	155
		compound **IV**		
N(1)−H(3)···O(1)	0.90	2.05	2.834(7)	145
N(1)−H(3)···O(3)	0.90	2.58	3.341(6)	143
N(1)−H(4)···O(4)	0.90	1.79	2.691(6)	175
C(1)−H(1)···O(3)	0.97	2.30	3.177(8)	149
		compound **V**		
N(2)−H(9)···O(8)	0.90	1.88	2.766(11)	169
N(2)−H(10)···O(2)	0.90	1.94	2.836(13)	174
N(1)−H(11)···O(10)	0.90	1.86	2.744(11)	168
N(1)−H(12)···O(6)	0.90	1.96	2.864(12)	177
N(3)−H(17)···O(10)	0.90	1.84	2.736(12)	178
N(3)−H(18)···O(4)	0.90	2.02	2.799(11)	144
O(4)−H(20)···O(8)	0.82	1.79	2.506(10)	145
O(12)−H(30)···O(100)	0.82	1.86	2.670(11)	171
		compound **VII**		
O(4)−H(4)···O(200)	0.82	2.26	3.077(8)	175
N(1)−H(30)···O(12)	0.89	1.95	2.828(7)	167
N(1)−H(32)···O(100)	0.89	2.04	2.926(8)	171
N(2)−H(39)···O(3)	0.90	1.94	2.827(6)	166
N(2)−H(40)···O(11)	0.90	1.97	2.846(7)	164
N(3)−H(47)···O(200)	0.89	1.97	2.834(9)	164
N(3)−H(48)···O(2)	0.89	2.34	3.125(7)	147
O(100)−H(101)···O(5)	0.85	1.97	2.799(8)	167
O(200)−H(201)···O(8)	0.84	2.00	2.793(9)	156
O(200)−H(202)···O(5)	0.85	2.41	3.160	147
C(1)−H(34)···O(3)	0.97	2.51	3.454(8)	164
C(3)−H(38)···O(100)	0.97	2.58	3.513(9)	162
C(5)−H(43)···O(12)	0.97	2.56	3.526(8)	176
C(6)−H(45)···O(100)	0.97	2.47	3.409(9)	162
		compound **VIII**		
N(1)−H(2)···O(3)	0.89	2.04	2.839(7)	148
N(1)−H(3)···O(11)	0.89	2.01	2.879(7)	166
O(8)−H(8)···O(2) intra	0.82	1.66	2.467(6)	169
N(2)−H(10)···O(1)	0.90	1.84	2.708(7)	163
N(2)−H(11)···O(12)	0.90	1.90	2.746(7)	156
N(3)−H(18)···O(7)	0.89	1.97	2.842(7)	166
N(3)−H(19)···O(5)	0.89	2.06	2.884(7)	153
N(3)−H(20)···O(10)	0.89	1.98	2.838(7)	163
O(100)−H(101)···O(2)	0.85	1.96	2.789(12)	162
O(100)−H(101)···O(200)	0.84	1.95	2.72(2)	150
C(2)−H(6)···O(10)	0.97	2.60	3.554(8)	170

Results

Zero-Dimensional Zinc Arsenate. *$[C_6N_4H_{21}][Zn(HAsO_4)_2(H_2AsO_4)]$, **I**.* The asymmetric unit contains 26 non-hydrogen atoms of which one zinc and three arsenic atoms are crystallographically distinct. The zinc atom is tetrahedrally coordinated by four oxygen-atom neighbors with an average Zn−O bond distance of 1.930 Å. The average O−Zn−O bond angle is 109.4°. The Zn atoms are connected to As atoms via As−O−Zn bridges with an average angle of 132.4°. Of the three independent As atoms, As(1) and As(3) form one As−O−Zn linkage and possess three

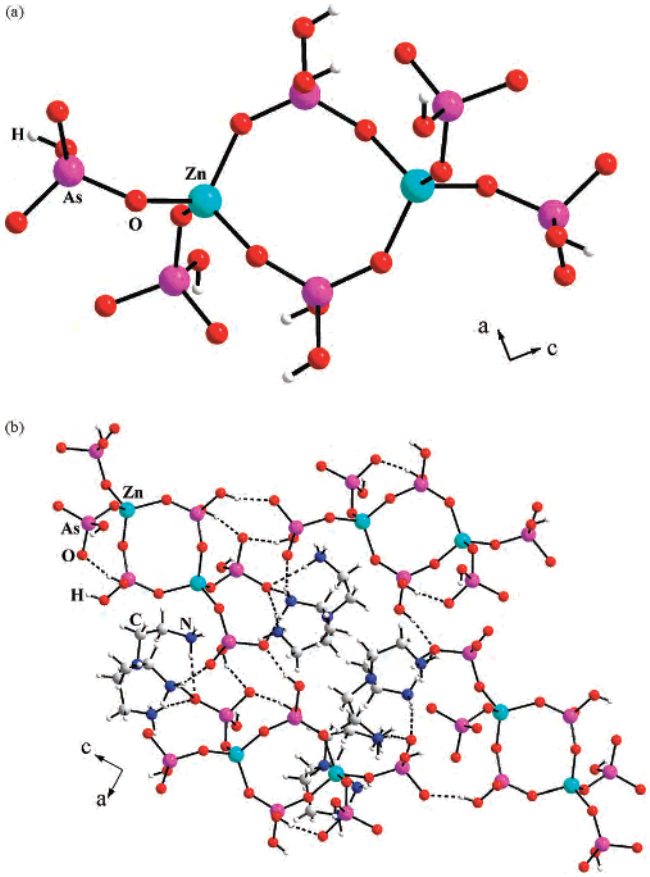

Figure 1. (a) Structure of the zinc arsenate, **I**. (b) Figure shows the packing arrangement of **I**. Dotted lines represent possible hydrogen-bond interactions.

terminal As−O bonds and As(2) has two As−O−Zn linkages and two terminal As−O bonds. The As−O bond distances are in the range of 1.647(3)−1.727(2) Å (av. As−O = 1.676 Å), and the O−As−O bond angles have an average angle of 109.4°. As(1)−O(4), As(2)−O(7), As(2)−O(8), and As(3)−O(12) with distances of 1.727(2), 1.6792(12), 1.6981(11), and 1.7125(12) Å, respectively, are As−OH linkages.

The structure of **I** consists of four-membered rings formed by the vertex linkages between ZnO_4 and $AsO_2(OH)_2$ tetrahedra. Two $AsO_3(OH)$ units hang from the Zn center to complete the zero-dimensional molecular structure (Figure 1a). The molecular unit is stabilized by intra- and intermolecular H-bond interactions through O−H···O, N−H···O, and C−H···O hydrogen bonds (Figure 1b, Table 4). To the best of our knowledge, **I** is the first amine templated zero-dimensional zinc arsenate.

One-Dimensional Zinc Arsenates. $[C_4N_2H_{12}][Zn(HAsO_4)_2]\cdot H_2O$, II, and $[C_5N_2H_{14}][Zn(HAsO_4)_2]\cdot H_2O$, III. The asymmetric unit of **II** and **III** contains 18 and 19 non-hydrogen atoms of which one zinc and two arsenic atoms are crystallographically independent. The zinc atoms are tetrahedrally coordinated by four oxygen-atom neighbors with an average Zn−O bond distance of 1.950 Å and an average O−Zn−O bond angle of 109.3° for **II** and **III**. The Zn atoms are connected to As atoms via the As−O−Zn bridges with an average angle of 125.2° for **II** and 128.0° for **III**. The arsenic atoms are connected to zinc via two As−O−Zn linkages and possess two terminal As−O bonds. The

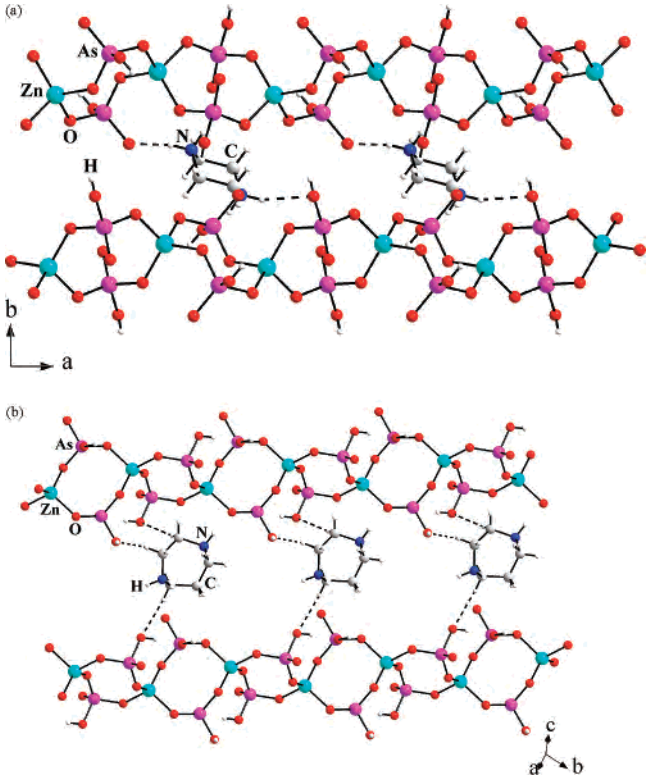

Figure 2. (a) One-dimensional chain structure observed in the zinc arsenate, $[C_4N_2H_{12}][Zn(HAsO_4)_2]\cdot H_2O$, **II**. (b) One-dimensional chain structure observed in the zinc arsenate, $[C_5N_2H_{14}][Zn(HAsO_4)_2]\cdot H_2O$, **III**. Note that the chains in **III** are more distorted. Dotted lines represent possible hydrogen-bond interactions.

As−O bond distances have an average value of 1.682 Å, and the O−As−O bond angles have an average value of 109.4° for **II** and **III**. The As(1)−O(4) and As(2)−O(8) bonds with distances of 1.724(5) and 1.709(5) Å for **II** and 1.726(4) and 1.712(3) for **III** are As−OH linkages.

The structures of both compounds are similar and consist of ZnO_4 and $HAsO_4$ units connected through their oxygen vertices to form the four-membered rings, which are linked through the corners forming a one-dimensional chain structure. The protonated amine molecules occupy the interchain spaces and participate in hydrogen-bond interactions. Thus, the 1D chain structures are stabilized via O−H···O-, N−H···O-, and C−H···O-type hydrogen bonds (Figure 2, Figure S10 and S11).

Two-Dimensional Zinc Arsenate. $[C_4N_2H_{12}][Zn(AsO_4)]_2$, IV. The asymmetric unit contains 9 non-hydrogen atoms of which one Zn and one As atom are crystallographically independent. The Zn atoms are tetrahedrally coordinated by four oxygen neighbors with an average Zn−O bond distances of 1.963 Å and O−Zn−O bond angles of 109.2°. The As atom is connected to the Zn atom via four As−O−Zn linkages with an average angle of 121.4°. The As atom is tetrahedrally coordinated with an average As−O bond distance of 1.668 Å and O−As−O bond angles of 109.4°. There are no terminal As−O linkages in this structure.

The structure consists of strictly alternating ZnO_4 and AsO_4 tetrahedral units connected through their vertices forming a two-dimensional structure. The unique feature of this structure is that all the tetrahedral corners are connected with each

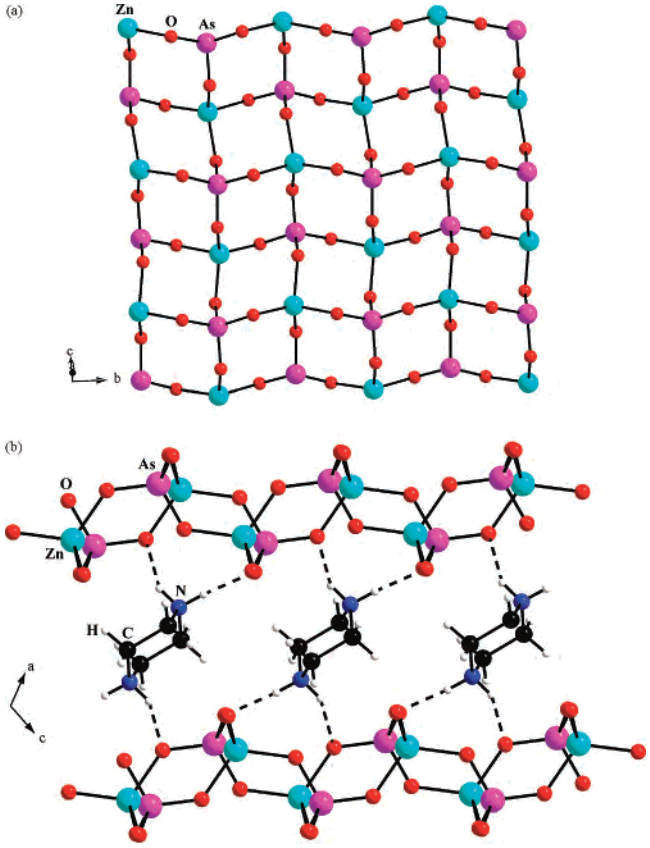

Figure 3. (a) Fully four-connected net observed in $[C_4N_2H_{12}][Zn(AsO_4)]_2$, **IV**. (b) Arrangement of layers in **IV**. The dotted lines represent possible hydrogen-bond interactions.

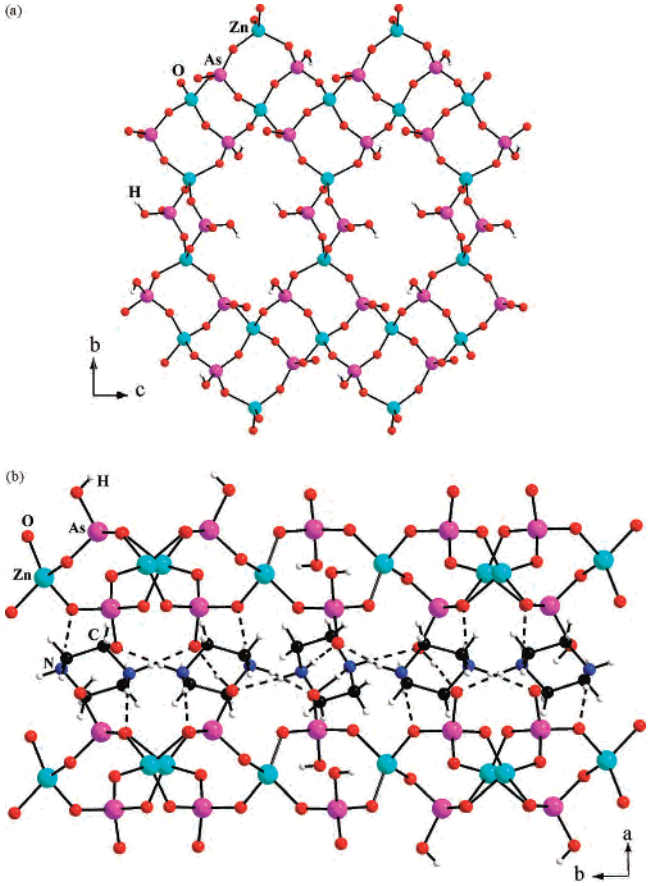

Figure 4. (a) Single-layer $[C_4N_2H_{12}]_{1.5}[Zn_2(AsO_4)(HAsO_4)_2]\cdot H_2O$, **V**. Note the zigzag ladder arrangement and the bifurcation by $HAsO_4$ units to form the 12-membered aperture. (b) Arrangement of the layers. Dotted lines represent possible hydrogen-bond interactions.

other, which gives rise to a four-connected 2D net (Figure 3a). The layers, which are anionic, are separated by the presence of protonated piperazinium cations. The layers are stacked in a *AAAA*... fashion (Figure 3b). The structure is stabilized by the C−H···O and N−H···O hydrogen-bond interactions (Table 4). To the best of our knowledge, this is the first amine-templated four-connected net in a two-dimensional structure, though a similar layered structure has been discovered in a zinc arsenate, $NaZnAsO_4\cdot 2H_2O$.[10a]

$[C_4N_2H_{12}]_{1.5}[Zn_2(AsO_4)(HAsO_4)_2]\cdot H_2O$, V. The asymmetric unit contains 27 non-hydrogen atoms of which two zinc and three arsenic atoms are crystallographically independent. The Zn atoms are tetrahedrally coordinated with an average Zn−O bond distance of 1.959 Å and average O−Zn−O bond angle of 109.4°. The zinc atoms are connected to the arsenic atoms via As−O−Zn bonds with an average angle of 131.2°. Of the three arsenic atoms, As(1) and As(3) form three As−O−Zn linkages and possess one terminal As−O bond and As(2) has four As−O−Zn bonds. The As−O bond distances are in the range 1.649(7)−1.723(7) Å (av. As−O = 1.684 Å), and the O−As−O bond angles have an average value of 109.4°. The As(1)−O(4) and As(3)−O(12) linkages with distances of 1.723(7) and 1.718(7) Å, respectively, are As−OH groups.

The structure consists of ZnO_4, AsO_4, and $HAsO_4$ tetrahedral units connected through their vertices, giving rise to a layered structure with 12-membered bifurcated ring apertures (Figure 4a). The other way to describe the structure is to consider ZnO_4, AsO_4, and $HAsO_4$ units linked together forming a zigzag one-dimensional ladder structure, which are connected through $HAsO_4$ units forming the bifurcated layer. The piperazinium cations along with the lattice water molecules occupy the inter-lamellar spaces. The layers are arranged in a *AAAA*... fashion (Figure 4b). Moderate hydrogen-bond interactions involving the layers and amine molecules have been observed (Table 4).

$[C_6N_4H_{21}]_6[Zn_{12}(HAsO_4)_{21}]$, VI. The asymmetric unit of **VI** contains 177 non-hydrogen atoms of which 12 zinc and 21 arsenic atoms are crystallographically independent. The Zn atoms have four and five coordination with respect to the oxygens. The Zn atoms with tetrahedral coordination have average Zn−O bond distances of 1.947 Å and O−Zn−O angles of 109.4°. Of the 12 Zn atoms, 3 Zn atoms, Zn(3), Zn(4), and Zn(11), have five coordination with their oxygen neighbors with average Zn−O bond distances of 2.047 Å and O−Zn−O angles of 106.4°, forming a trigonal bipyramidal arrangement. The Zn atoms, Zn(3), Zn(4), and Zn(11), have five coordination with their oxygen neighbors forming a trigonal bipyramidal arrangement. All Zn atoms are connected to the arsenic atoms via Zn−O−As linkages with an average bond angle of 126.1°. The As−O bond distances have an average value of 1.677 Å and the O−As−O angle a value of 109.4°. The average terminal

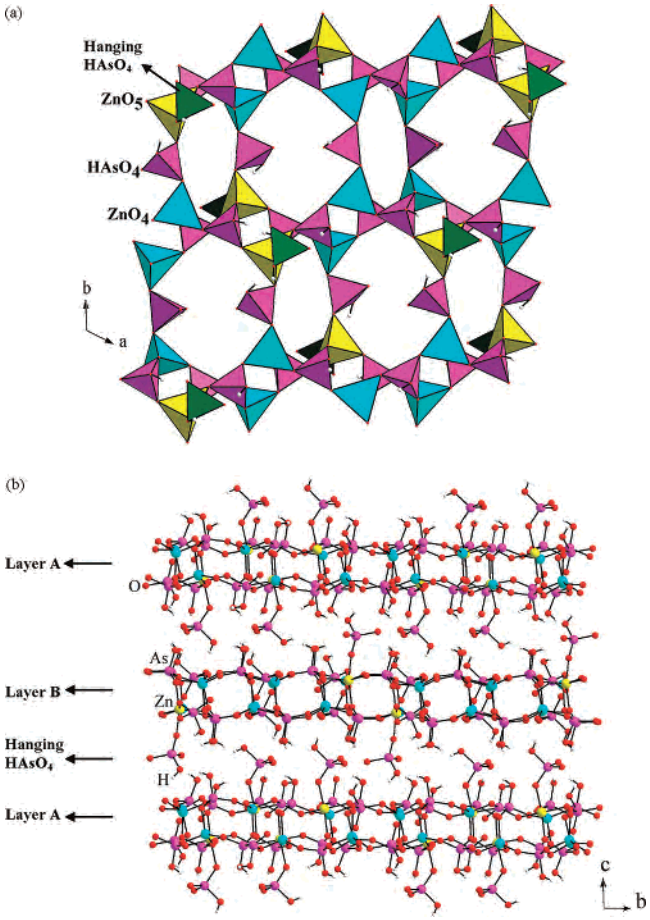

Figure 5. (a) View of a single layer in $[C_6N_4H_{21}]_6[Zn_{12}(HAsO_4)_{21}]$, **VI**. (b) Arrangement of the layers. Note the hanging $HAsO_4$ groups. The amine molecules are not shown for clarity.

distance of As−OH and As═O is 1.712 and 1.654 Å, respectively.

The structure consists of ZnO_4, ZnO_5, and $HAsO_4$ polyhedral units connected through the vertices. In spite of the larger number and varying coordinations around the Zn atoms, there are no Zn−O−Zn linkages in this structure. The connectivity between these units gives rise to a two-dimensional layer with 4-, 8-, and 12-membered aperture (Figure 5a). The pentacoordinated Zn atoms are bonded with $HAsO_4$ units, which hang into the inter-lamellar region. The inter-lamellar region is also occupied by the protonated TREN molecules. The layers are arranged in a *ABAB*... fashion. The presence of terminal $HAsO_4$ units along with the TREN molecules in the interlayer spaces gives rise to a large number of O−H···O-, N−H···O-, and C−H···O-type hydrogen-bond interactions (Figure 5b and Table S2).

$[C_6N_3H_{20}][Zn_2(AsO_4)(HAsO_4)_2]\cdot 2H_2O$, VII and VIII. Compounds **VII** and **VIII** have the same molecular formula and comparable structures with 28 non-hydrogen atoms in their asymmetric units of which 2 zinc and 3 arsenic atoms are crystallographically independent. Both compounds have the Zn atoms in tetrahedral coordination with Zn−O bond distances in the range 1.929(4)−1.975(4) Å (av. Zn−O = 1.953 Å for **VII** and 1.947 Å for **VIII**), and the O−Zn−O bond angles have an average value of 109.1° for **VII** and 109.3° for **VIII**. The Zn atoms are connected to As via the oxygen bridges with an average Zn−O−As bond angle of 128.47°. The As atoms have As−O bond lengths in the range 1.659(4)−1.723(4) Å (av. As−O = 1.686 Å for **VII** and 1.681 Å for **VIII**), and O−As−O bond angles have an average value of 109.4° in both compounds. The longer As−O distances, again, correspond to As−OH bonds [As(1)−O(4) = 1.723(4) Å and As(2)−O(8) = 1.719(4) Å] (Table 3).

Compounds **VII** and **VIII** can be considered as polymorphs. Both compounds are formed by strictly alternating ZnO_4 and $AsO_3(OH)$ tetrahedral units, connected through their vertices. The connectivity gives rise to ladder-like one-dimensional units, which are further bonded through the four-membered ring, giving rise to a two-dimensional structure with apertures bound by 8-T atoms (T = Zn, As). The tetrahedral $AsO_3(OH)$ groups which are bound to the Zn atom hang from the layer and protrude into the inter-lamellar region wherein the protonated amine molecules along with water molecules also reside (Figure 6a). To the best of our knowledge, this is the first observation of polymorphic structures in amine-templated zinc arsenates. The presence of $HAsO_4$ units along with the amine and water molecules in the interlayer spaces give rise to O−H···O-, N−H···O, and C−H···O-type hydrogen-bond interactions (Figure 6b, Table 4).

Investigations on the Reactivity of the Zero-Dimensional Molecular Zinc Arsenate, I. One of the important compounds isolated during the present study is the zero-dimensional monomer zinc arsenate, $[C_6N_4H_{21}][Zn(HAsO_4)_2(H_2AsO_4)]$, **I**. It has been shown by Rao and co-workers that the zero-dimensional zinc phosphates with four-membered rings could be the basic building block for structures of higher dimensionality.[17d,f] In light of this, isolation of such a structure in the family of arsenates attains significance. Similar to the studies of the monomer phosphate structure, we desired to investigate the reactivity of the monomer arsenate phase under a variety of reaction conditions. We listed the representative reaction conditions employed for the transformation studies in Table 5.

During the transformation studies many phases appear to form as seen by powder XRD patterns (Figure S12−S15). From the studies on phosphate compounds it is proposed that the fundamental step in the transformation of zero-dimensional monomer is the facile deprotonation of the terminal −OH group. Thus, one can use many different approaches for this step. In our experiments we find that use of $Zn(OAc)_2\cdot 2H_2O$ along with **I** under hydrothermal conditions led to formation of condensed zinc arsenate $Zn_2(AsO_4)OH$ (ICDD-76-0895). The conjugate base of the acetic acid, $(CH_3COO)^-$, probably acted as the deprotonating agent.

(17) (a) Harrison, W. T. A.; Bircsak, Z.; Hannooman, L.; Zhang, Z. *J. Solid State Chem.* **1998**, *136*, 93. (b) Chidambaram, D.; Neeraj, S.; Natarajan, S.; Rao, C. N. R. *J. Solid State Chem.* **1999**, *147*, 154. (c) Choudhury, A.; Natarajan, S.; Rao, C. N. R. *Inorg. Chem.* **2000**, *39*, 4295. (d) Ayi, A. A.; Choudhury, A.; Natarajan, S.; Neeraj, S.; Rao, C. N. R. *J. Mater. Chem.* **2001**, *11*, 1181. (e) Choudhury, A.; Neeraj, S.; Natarajan, S.; Rao, C. N. R. *J. Mater. Chem.* **2001**, *11*, 1537. (f) Rao, C. N. R.; Natarajan, S.; Choudhury, A.; Neeraj, S.; Ayi, A. A. *Acc. Chem. Res.* **2001**, *34*, 80.

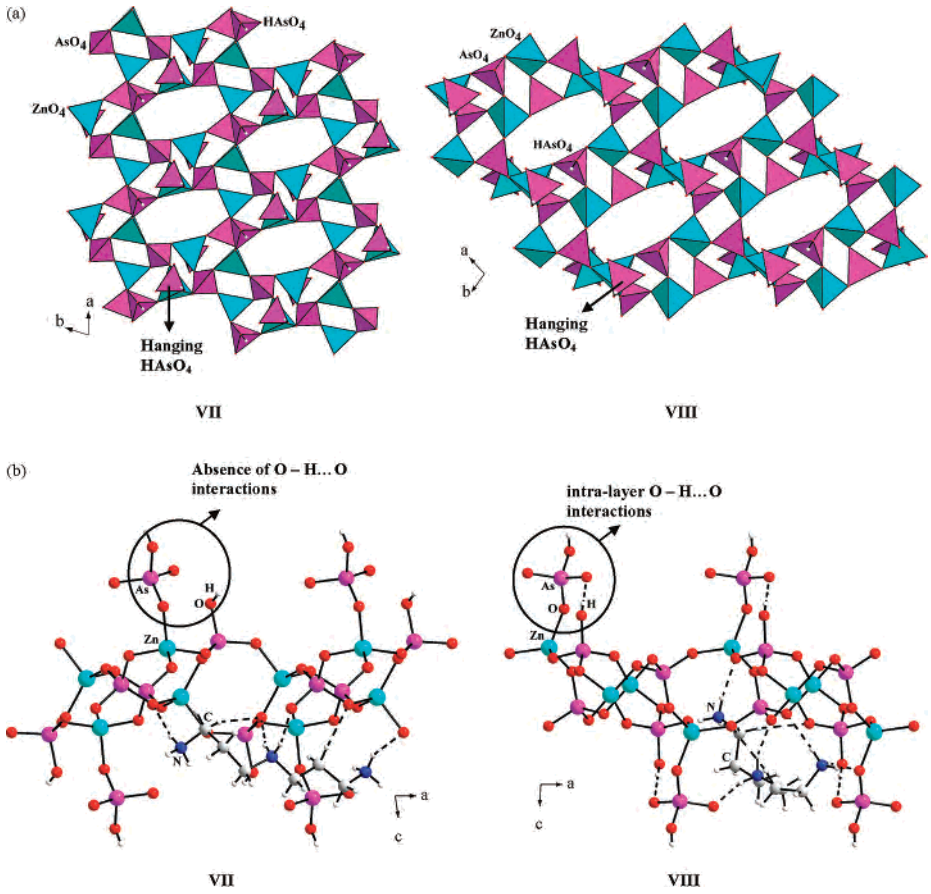

Figure 6. (a) Polyhedral view of the single layer in the zinc arsenates, $[C_6N_3H_{20}][Zn_2(AsO_4)(HAsO_4)_2]\cdot 2H_2O$, **VII** and **VIII**. Note the subtle differences in the aperture sizes between the structures. (b) View of a portion of the structure explicitly showing the subtle difference in the hydrogen-bond interaction between the two polymorphic zinc arsenates, **VII** and **VIII**. Note formation of the intralayer O−H···O hydrogen bonds in **VIII**.

Table 5. Experimental Conditions Employed for Study of the Transformation of the Zero-Dimensional Zinc Arsenate, $[C_6N_4H_{21}][Zn(HAsO_4)_2(H_2AsO_4)]$, **I**

no.	composition	temp (°C)	time (h)	pH	product
1	1**I** + $300H_2O$	180	72	6.0	$Zn_2(AsO_4)(OH)$ (ICDD-76-0895)
2	1**I** + $1Zn(OAc)_2\cdot 2H_2O$ + $300H_2O$	150	48	4.0	$Zn_2(AsO_4)(OH)$ (ICDD-76-0895)
3	1**I** + $2Zn(OAc)_2\cdot 2H_2O$ + $300H_2O$	110	96	4.0	$Zn_2(AsO_4)(OH)$ (ICDD-76-0895)
4	1**I** + $1CH_3COOH$ + $300H_2O$	110	96	4.0	$Zn_2(AsO_4)(OH)$ (ICDD-76-0895)
5	1**I** + 1DABCO+ $200H_2O$	180, 200	72, 24	7.0	$(NH_3CH_2CH_2NH_3)_{0.5}.ZnAsO_4$[10b]
6	1**I** + 1EN + $200H_2O$	150 or 180	48	8.0	$(NH_3CH_2CH_2NH_3)_{0.5}.ZnAsO_4$[10b]
7	1**I** + 1TREN + $200H_2O$	150 or 180	72	7.0	uncharacterized phase[a]
8	1**I** + 1PIP+ $200H_2O$	150	72	7.0	**V** + $[C_4N_2H_{12}]_2[Zn_7(AsO_4)_6(H_2O)_2$[10f]
9	1**I** + 1PIP+ 22THF + $200H_2O$	150	72	7.0	**V** + $[C_4N_2H_{12}]_2[Zn_7(AsO_4)_6(H_2O)_2$[10f]
10	1**I** + 1Imidazole + 22 THF + $200H_2O$	150, 180	72, 48	7.0	VI
11	1**I** + 1Imidazole + 22 THF + $300H_2O$	100	48	7.0	VI

[a] A mixture of phases containing **I**, **VI**, and other unknown phases.

We observed a similar behavior when we reacted acetic acid with **I**. Use of organic amine, on the other hand, appears to favor formation of higher dimensional zinc arsenate structures, some of which have already been isolated independently.

Use of piperazine with **I** under hydrothermal conditions forms a three-dimensional zinc arsenate, $[C_4N_2H_{12}]_2[Zn_7(AsO_4)_6(H_2O)_2]$,[10f] and the use of *en* gives rise to another three-dimensional structure, $[C_2N_2H_{10}]_{0.5}\cdot ZnAsO_4$.[10b] Use of DABCO forms the same compound that was isolated using *en*, $[C_2N_2H_{10}]_{0.5}\cdot ZnAsO_4$.[10b] It is likely that the DABCO molecules decomposed during the transformation reaction giving rise to *en*. This decomposition behavior of organic amine molecules under hydrothermal conditions is known.[18] In all these cases, we observed exchange of an original amine molecule of the monomer, TREN, with the amine used for deprotonation. A similar behavior has also been seen during the transformation studies of zero-dimensional zinc phosphate.[17d] Use of imidazole, on the other hand, gave rise to the layered zinc arsenate, $[C_6N_4H_{21}]_6[Zn_{12}(HAsO_4)_{21}]$, **VI**, isolated in this study. Since during this transformation we did not observe any amine exchange, we wanted to investigate the probability of any intermediate structure.

Thus, we carried out a time-dependent study at 100 °C. The results indicated that the layered compound, **VI**, forms

(18) Natarajan, S.; Cheetham, A. K. *J. Solid State Chem.* **1997**, *134*, 207.

Scheme 1. Schematic Showing a Possible Pathway for Formation of Other Structures Isolated in the Present Study from the Basic Building Unit, the Four-Membered Ring Monomer, **I**

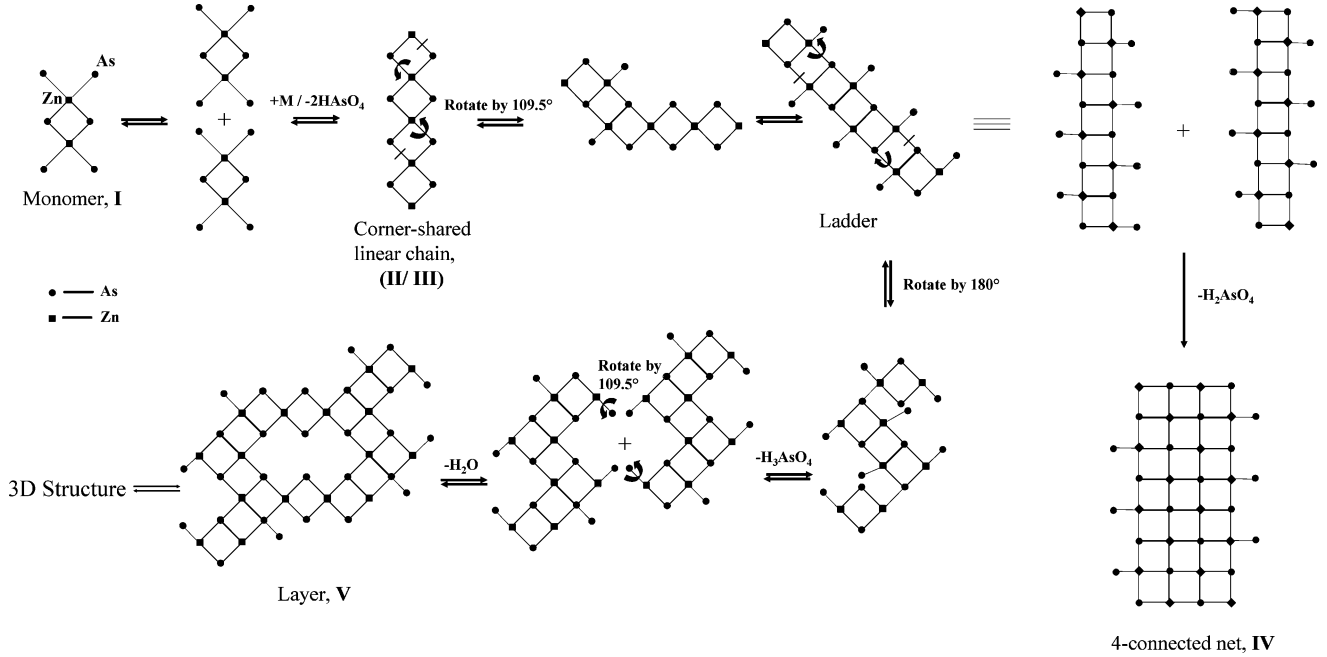

after about 24 h (Figure S13), indicating that transformation of the monomer to the layer structure is facile in the presence of imidazole.

This observation prompted us to study the transformation reactions of the zero-dimensional zinc arsenate further under a variety of conditions, especially lower temperature (room temperature). For this study, we employed piperazine. A composition of 1**I**:1PIP:480H_2O, at room temperature gave good-quality crystals after 48 h. The single-crystal structural studies show that the structure is the one-dimensional corner-shared chain structure, $[C_4N_2H_{12}][Zn(HAsO_4)_2]\cdot H_2O$, **II**, observed in the present study. We also carried out a time-dependent study at room temperature to understand the evolution of the phase using piperazine at room temperature. The results indicate that **I** transforms immediately to **II** (∼30 min), (Figure S14). In order to understand this reaction better and investigate the possible correlation between the concentrations of molecular zinc arsenate and piperazine, we also carried out a concentration-dependent study. For this we varied the molar concentration of piperazine from 0.25 to 2.0, keeping the concentration of **I** as 1 M. The results again indicate that only the 1D zinc arsenate structure is the transformed phase (Figure S15). Similar studies using TREN molecules as the added amine appear to form only the layer structure, $[C_6N_4H_{21}]_6[Zn_{12}(HAsO_4)_{21}]$, **VI**.

The above studies clearly indicate that the monomer zinc arsenate, **I**, is reactive. Formation of one-, two-, and three-dimensionally extended structures from the four-membered ring monomer appears to be facile. One can visualize the formation of such structures from the monomer, which is presented schematically in Scheme 1.

Discussion

Eight new zinc arsenate compounds exhibiting a hierarchy of structures have been prepared, employing hydro/solvothermal methods, as good-quality single crystals. The reactions themselves are quite simple in most cases and have been carried out at relatively mild conditions (<150 °C) (Table 1). During the course of the present studies we have been able to isolate the first amine-templated molecular zinc arsenate, fully four-connected two-dimensional layered zinc arsenate, as well as the polymorphic zinc arsenate phases. The subtle variations in the observed structures are likely to result from the differences in the experimental conditions such as the composition, time, and temperature (Table 1), but we are not yet in a position to relate and correlate these aspects.

Compounds **I** and **VI** have been prepared by the same amine molecules, TREN, the polymorphic structures of **VII** and **VIII** using DPTA. Use of piperazine produced compounds **II**, **IV**, and **V**, while a related amine, homopiperazine, gave compound **III**. Formation of different structures of varying dimensionalities using the same amine molecules has been well documented in the literature,[17c] and it is not surprising that we have also been able to prepare a number of compounds using the same amine molecules.

Of the eight compounds synthesized during the present study, preparation of the zinc arsenate monomer is noteworthy as it is the first example of a zero-dimensional structure in the family of templated arsenates. By varying the synthetic conditions we also prepared a two-dimensional layered compound, **VI**. Since the four-membered ring appears to be the fundamental building unit in framework solids, one can visualize formation of the layered structure (**VI**) from the monomer (**I**), though the process must involve breaking and making of many bonds. The second simplest member in the family of phosphates and other related compounds is the one-dimensional corner-shared chain structure, which was also isolated during the course of the present study. The one-dimensional ladder structure, however, was not isolated in

the present study, though such structures have been known among the zinc phosphates.[17a−c]

One of the important structures, isolated in the present study, is the fully four-connected layer structure, **IV**. From the known zeolitic structures, it is well-established that the three-connected nets usually form two-dimensional structures and four-connected nets form three-dimensional ones.[19] Tetrahedral atoms forming two-dimensional structures usually have interruptions and are never fully four-connected.[20] Under these circumstances isolation of a four-connected 2D structure in **IV** is noteworthy. A similar layered structure has been isolated recently in a sodium zinc arsenate, $NaZnAsO_4 \cdot 2H_2O$,[10a] with the Na^+ ions occupying the interlayer spaces. In **IV**, the interlayer spaces are occupied by the protonated piperazine cations. The present compound along with the $NaZnAsO_4 \cdot 2H_2O$ compound represent the only known examples of the four-connected 2D net, and **IV** is unique as it has been prepared in the presence of the organic amine molecules.

During the course of this study we also isolated the first known polymorphic structures in open-framework zinc arsenates. Polymorphism as a phenomenon is common among organic systems,[21] and isolating such structures in amine-templated framework structures is not known. Formation of polymorphic structures in **VII** and **VIII** probably has its origin in the subtler forces within the solids−hydrogen-bond interactions. Careful analysis of the hydrogen-bond interactions in both structures reveals that both intra- and interlayer hydrogen bonds have been observed in **VIII**, while only the interlayer hydrogen bonds have been observed in **VII**. The hydrogen bond, O(8)−H(8)···O(2), with a O−O contact distance of 2.467(6) Å and O−H···O angle of 169° appears to be unique and possibly causes the structure of **VIII** to arrange differently compared to **VII**. Polymorphism based on such hydrogen-bond interactions have been observed recently in the mineral zinc phosphate hopeite, $Zn_3PO_4 \cdot 4H_2O$.[22]

The present study contains structures of different dimensionalities, and it is pertinent to discuss the importance of hydrogen-bond interactions in the structural stability of the phases. It has been well documented in the literature that the hydrogen bonds play a crucial role in the stability of lower dimensional structures.[17d,e] In the present compounds O−H···O and N−H···O interactions appear to be dominant (Table 4 and Table S2). The O−O (donor−acceptor) distances are in the range 2.467−3.160 Å for the O−H···O interactions (av. 2.594 Å for **I**, 2.716 Å for **II**, 2.684 Å for **III**, 2.588 Å for **V**, 2.619 Å for **VI**, 2.957 Å for **VII**, 2.658 Å for **VIII**), and the O−H···O bond angles are in the range 144−175.0° (av. 157.2° for **I**, 159.3° for **II**, 164.5° for **III**, 158.0° for **V**, 159.8° for **VI**, 161.25° for **VII**, 160.3° for **VIII**). Similarly for the N−H···O interactions we find N···O distances in the range 2.658−3.431 Å (av. 2.830 Å for **I**, 2.845 Å for **II**, 2.955 Å for **IV**, 2.790 Å for **V**, 2.995 Å for **VI**, 2.897 Å for **VII**, 2.819 Å for **VIII**) and N−H···O bond angles in the range 143.0−178.0° (av. 162.6° for **I**, 166.3° for **II**, 154.3° for **IV**, 168.3° for **V**, 157.2° for **VI**, 163.1° for **VII**, 159.2° for **VIII**). In addition, we also observed significant C−H···O interactions in some of the compounds. Thus, C−H···O interactions have been observed in **I**, **III**, **IV**, **VI**, **VII**, and **VIII** with C···O distances in the range 2.717−3.554 Å (av. 3.397 Å for **I**, 2.980 Å for **III**, 3.177 Å for **IV**, 3.397 Å for **VI**, 3.475 Å for **VII**, 3.554 Å for **VIII**) and C−H···O bond angles in the range 145.0−176.0° (av. 164.0° for **I**, 163.1° for **III**, 149.0° for **IV**, 158.5° for **VI**, 166.0° for **VII**, 170.0° for **VIII**). Though the strength and number of C−H···O interactions are considerably less, the importance of such interactions toward the structural stability could be significant. The importance of C−H···O interactions in the supramolecular assemblies or organic compounds has been well described, but the role of such interactions has not been developed for framework structures.

In many of the low-dimensional structures the hydrogens of the water molecules or the hydrogens attached to the nitrogens of the organic amine molecules interact with the framework oxygens, giving rise to O−H···O- and N−H···O-type hydrogen bonds. In the presence of the stronger interactions described above, the C−H···O hydrogen bonds, at best, can have a secondary contribution. Combination of hanging arsenates and longer amine molecules in some of the structures gave rise to significant C−H···O-type hydrogen bonds in the present compounds. It is likely that such interactions would be necessary for the overall structural stability, especially in the case of molecular and one-dimensional structures. Further work is necessary for evaluating the exact role of such weak interactions in the formation and stability of framework structures.

Acknowledgment. S.N. thanks the Department of Science and Technology (DST), Government of India, for the award of a research grant and a RAMANNA fellowship. V.K.R. thanks the Council of Scientific and Industrial Research (CSIR), Government of India, for the award of a research fellowship.

Supporting Information Available: Important bond distances and hydrogen-bond interactions observed in compounds **II**, **III**, and **VI** (Tables S1 and S2); powder X-ray patterns of (a) simulated and (b) experimental **I** (Figure S1), **IV** (Figure S2), **VII** (Figure S3), and **VIII** (Figure S4); TGA of **I**, **III**, and **VI** (Figure S5), and the powder XRD patterns of the corresponding calcined samples (Figure S6−S8); IR spectra of **I**, **III**, **IV**, and **VI** (Figure S9); hydrogen-bond interactions of the lattice water with the framework oxygens in **II** and **III** (Figure S10 and S11); powder X-ray patterns of transformed products of **I** with *en* (Figure S12), with imidazole varying the time (Figure S13), with PIP varying the time (Figure S14) and concentration (Figure S15). This material is available free of charge via the Internet at http://pubs.acs.org.

IC7014594

(19) Smith, J. V. *Chem. Rev.* **1988**, *88*, 149.
(20) DeBord, J. R. D.; Haushalter, R. C.; Zubieta, J. *J. Solid State Chem.* **1996**, *125*, 270.
(21) (a) Bernstein, J.; Davey, R. J.; Henck, J. O. *Angew. Chem., Int. Ed.* **1999**, *38*, 3440. (b) Bernstein, J. *Polymorphism in Molecular Crystals*; Oxford Science Publications: Negev, 2002.
(22) Herschke, L.; Enkelmann, V.; Lieberwirth, I.; Wegner, G. *Chem. Eur. J.* **2004**, *10*, 2795.